POTENTIAL ROLE OF SOLAR VARIABILITY AS AN AGENT FOR CLIMATE CHANGE

CÉDRIC BERTRAND and JEAN-PASCAL VAN YPERSELE
Institut d'Astronomie et de Géophysique Georges Lemaître, Université Catholique de Louvain, Chemin du Cyclotron 2, B-1348 Louvain-la-neuve, Belgium
E-mail: cedric@astr.ucl.ac.be and vanypersele@astr.ucl.ac.be

Abstract. Numerical experiments have been carried out with a two-dimensional sector averaged global climate model in order to assess the potential impact of solar variability on the Earth's surface temperature from 1700 to 1992. This was done by investigating the model response to the variations in solar radiation caused by the changes in the Earth's orbital elements, as well as by the changes intrinsic to the Sun. In the absence of a full physical theory able to explain the origin of the observed total solar irradiance variations, three different total solar irradiance reconstructions have been used. A total solar irradiance change due to the photospheric effects incorporated in the Willson and Hudson (1988) parameterization, and the newly reconstructed solar total irradiance variations from the solar models of Hoyt and Schatten (1993) and Lean et al. (1995).

Our results indicate that while the influence of the orbital forcing on the annual and global mean surface temperature is negligible at the century time scale, the monthly mean response to this forcing can be quite different from one month to another. The modelled global warming due to the three investigated total solar irradiance reconstructions is insufficient to reproduce the observed 20th century warming. Nevertheless, our simulated surface temperature response to the changes in the Sun's radiant energy output suggests that the Gleissberg cycle (≈88 years) solar forcing should not be neglected in explaining the century-scale climate variations.

Finally, spectral analysis seems to point out that the 10- to 12-year oscillations found in the recorded Northern Hemisphere temperature variations from 1700 to 1992 could be unrelated to the solar forcing. Such a result could indicate that the eleven-year period which is frequently found in climate data might be related to oscillations in the atmosphere or oceans, internal to the climate system.

1. Introduction

One of the most fundamental quantities in relation to the terrestrial climate is the Sun's radiation. It follows that an important step in the analysis of the causes of climatic change is a study of the changes in the solar radiation received at the top of the atmosphere. Indeed, since the Sun is the principal energy source of the Earth's climatic system, it is natural to suspect variations in solar radiation as a possible source of climate variations at the secular time scale (Reid, 1991). There are two distinct causes of this variability of solar radiation. The first is related to the periodic changes in the Earth's orbital elements, which in turn influence the latitudinal and seasonal distribution of the solar energy received by the Earth (the so-called 'astronomical or Milankovitch effect'). These changes act with greatest

Climatic Change **43:** 387–411, 1999.

impact on time scales of 10,000 to 100,000 years and have been responsible, at least partly, for the major glacial–interglacial cycles that occurred during the Quaternary period (Berger, 1988).

The second source of variability of solar radiation comes from physical changes of the Sun itself; such changes occur on almost all time scales. Models of stellar evolution indicate that the solar luminosity has increased over geologic time. As hydrogen is converted to helium in the solar core, the rate of nuclear burning increases, causing the total solar irradiance to be some 20–30% higher today than it was at the time of the Earth's formation (Newman and Rood, 1977). At shorter time scale, changes in the Sun's radiant energy output have been confirmed by recent satellite measurements, at least on the time scale of the 11-year Schwabe solar cycle and shorter (Hickey et al., 1988; Willson and Hudson, 1988, 1991). These recent findings supplied, for the first time, a quantitative connection between solar activity, as measured in sunspot number, and the Sun's total output of radiative flux. During the last 11-year solar cycle, the magnitude of the irradiance variation is of the order of 0.1% of the solar constant.

At the Earth's mean distance from the Sun, the irradiance normal to the Earth-Sun line is approximately 1368 Wm^{-2}. Because the Earth's surface area is four times its cross-section and 30% of the sunlight is reflected back to space without being absorbed, the mean solar heating of the Earth is $\approx$240 Wm^{-2}. A change of solar forcing irradiance by 0.1% is therefore a climate forcing of $\approx$0.24 Wm^{-2}. By comparison, the best available estimation of the radiative forcing due to the increase of anthropogenic greenhouse gases from pre-industrial (1880) to present-day concentrations is about 2.4 Wm^{-2} (Houghton et al., 1996).

While it is generally accepted that such variations are unlikely to have significant impact on climate, partly due to the small amplitude (the associated radiative forcing is typically 10% of the present day greenhouse forcing as seen above), and partly due to the damping of such 'short-term' variations by the thermal inertia of the oceans (Hoffert et al., 1988; Reid, 1991; Smits et al., 1993), changes in solar activity are still regularly forwarded as an hypothesis to explain the observed warming over the last century. Nevertheless, the support of such claim is largely statistical in terms of good correlations and high explained variance, as physical relationships are unknown or speculative. The most illustrative study of this kind is the paper published by Friis-Christensen and Lassen (1991) in which they demonstrated the existence of a strong correlation between the length of the well-known 11-year solar cycle and the Northern Hemisphere land mean surface temperature since 1860. This lead these autors to suggest that the anthropogenic enhancement of the greenhouse effect is virtually absent from the temperature record and that almost all the observed decadal temperature variation is due to variations in solar activity. This was not the first study of the Sun-weather and Sun-climate relation but never before had such strong correlation been found. Since then, this paper has been criticized both on statistical and physical grounds (e.g., Schlesinger and Ramankutty, 1992; Kelly and Wigley, 1992; van Ulden and van Dorland, 1998).

Using an upwelling-diffusion Energy-Balance Model (EBM) to simulate the Earth's surface temperature response to the anthropogenic climate forcings and to solar-irradiance variations of the form posited by Friis-Christensen and Lassen (1991), Schlesinger and Ramankutty (1992) found strong circumstancial evidence that there have been intercycle variations in solar irradiance which have contributed to the observed temperature changes since 1865, but their model calculations indicated, also in agreement with Kelly and Wigley (1992), that since the nineteenth century greenhouse gases have been the dominant contributor to the observed temperature changes. Moreover, in their more recent study, van Ulden and van Dorland (1998) clearly showed that the positive correlation found by the two Danish scientists is artifically enhanced by the use of a poorly performing time filter and a questionable extrapolation of observations leading to a highly distorted record of solar cycle length that is unreliable after 1975.

Moreover, statistical correlations (which by themselves can never prove a physical connection between solar activity variations and climate) imply only a minor role for the physical basis of the greenhouse theory although a dominance of solar variability over greenhouse forcing can only be explained by a large, and yet unknown, positive feedback mechanism. To overcome this difficulty, some have argued that the climate sensitivity for solar forcing would be significantly larger than for other forcing agents. Such a possibility is offered by the recent result of Svensmark and Friis-Christensen (1997), in which they claim a large impact of the sunspot cycle on global temperatures. They found a high correlation between the cosmic ray intensities and the Earth's cloud cover as observed by satellites during the period 1980–1995. Galactic cosmic rays penetrate the Earth's atmosphere depths, causing ionisation of air particles. The flux of galactic cosmic rays varies inversely with solar activity, due to a shielding effect of solar wind, which varies in intensity in phase with the solar cycle.

There is at present no detailed understanding of the micro-physical mechanism that connect solar activity and Earth's cloud cover, although it is believed that ionisation affects the micro-physics of cloud formation (see e.g., Dickinson, 1975). The correlation has to be interpreted as a decrease of cloudiness with increasing solar activity (and an increase in cloudiness with decreasing solar activity). However, Svensmark and Friis-Christensen omitted to specify the altitude of the suggested cloud variation of 3%, which is crucial for the determination of the climate effects (Schneider, 1972). As an example, cirrus (high) cloud variations affect global temperatures, but with the disadvantage of having the wrong sign. Testing the Svensmark and Friis-Christensen cosmic ray – cloud cover hypothesis by use of a 1-D coupled radiative-convective atmosphere ocean model, van Dorland and van Ulden (1998) found that while some recent 11-year temperature fluctuations match the computed effects of the sunspots cycle, this response is out-of-phase with the observed fluctuations before 1950. Moreover, the observed long-term temperature trends are considerably larger, showing a much colder epoch before 1930, and warmer epochs around 1940 as well as in the last two decades.

More can probably be expected from the ultraviolet emissions from the Sun, in spite of the fact that the absolute fluxes of these energetic radiations are relatively small. One reason is that UV irradiance, which is more variable by at least an order of magnitude than longer-wavelength visible radiation, although energy-wise only containing 1% of the total radiation flux (Lean, 1989), may impact climate indirectly by modulating the ozone layer and hence the radiative and dynamical coupling of the stratosphere and the troposphere (Haigh, 1994). A model experiment (Haigh, 1996) investigating the role of UV and ozone variations on changes in tropopospheric circulation suggests that this leads to a non-negligible tropospheric response, resembling some of the statistically derived responses of connections between atmospheric circulation patterns and solar activity (e.g., Labitzke and van Loon, 1993, 1995).

Nevertheless, it is not at all certain that satellite measurements have captured the full range of the Sun's variability. The variation of the peaks in successive 11-year sunspot cycles show, for example, evidence of a periodicity of around 88 years often termed the Gleissberg cycle (Eddy, 1988); and over still longer time scales, there is evidence for protracted periods of enhanced activity and of extensive quiescence, for example, during the Maunder Minimum when, from 1645 to 1715, sunspots were essentially absent from the solar disc (Eddy, 1976). Since the attenuation caused by the oceans would be much less on century-scale fluctuations (Hoffert et al., 1980), the solar forcing would be therefore more important for understanding climate forcing on time-scales of centuries or more (Eddy and Oeschger, 1993). New estimates from solar models of the potential changes in solar variability hypothesize amplitudes in the order of 0.24–0.30% at the centennial time scales (Hoyt and Schatten, 1993; Lean et al., 1995). Calculation with climate models (Reid, 1991; Rind and Overpeck, 1993; Crowley and Kim, 1996; Cubasch et al., 1997) suggested that such changes could potentially cause surface temperature changes on the order of several tenths of a degree Celsius.

Forcing their GCM with a 0.24% irradiance reduction as estimated by Lean et al. (1992) for the Maunder Minimum Period, Rind and Overpeck (1993) simulated a cooling of 0.49 °C. However, current estimates of the global temperatures drop during the Maunder Minimum which coincided roughly with one of the coldest episodes of the Little Ice Age ranges from 1 to 1.5 °C colder than modern temperatures (e.g., Wigley and Kelly, 1990; Crowley and North, 1991; Bradley and Jones, 1993). This led therefore to suggest that a reduction of solar irradiance of 0.24% is too small to explain the cooler temperatures as a result of solar variability alone. More recently, Reid (1997) proposed a reconstructed historical irradiance variations scaled to cause an increase of 1 °C from the time of the Maunder Minimum to 1980. Using such a reconstruction based on climatic considerations, Reid (1997) concluded that the importance of solar variability as an agent in climate change over the last few decades may have been underestimated in recent studies.

The aim of this paper is therefore to investigate with a two-dimensional sector averaged global climate model the potential impact of the astronomical forcing and

the Sun's variability on the Earth's surface temperature over the last three centuries. Due to the lack of direct measurements of solar radiation on climatological time scale, this is done in the light of newly reconstructed solar total irradiance variations from solar models of Hoyt and Schatten (1993) (here after referenced as 'Sc.HS') and Lean et al. (1995) (here after 'Sc.LN') as well as by extending the best-fit relationship for the variation of total solar irradiance with sunspot number (Willson and Hudson, 1988) (here after 'Sc.WH').

Previous assessments of climate change that have considered possible effects of the Sun focused on multi-decadal and centennial time scales, assumed that the Schwabe radiation cycle is too short and its amplitude too small to have any significant effect on the climate system. Here, spectral analysis is applied to surface temperature time series simulated by the model in order to highlight their line frequencies and the associated amplitudes.

2. Solar Index Description and Comparison

Whatever the mechanisms of Sun-climate interactions may be, the assessment of the importance of solar variability in explaining climate change is limited primarily by our lack of knowledge of century-scale solar variability. Therefore, in the abscence of the necessary accurate long-term observations, the investigation of Sun-climate relations has to rely on proxy records of solar activity.

As quoted in the introduction, Reid (1997) based on climatic considerations (a temperature drop of about 1 °C from modern values during the Maunder Minimum) and taking into account the anthropogenic greenhouse gas forcing since the pre-industrial era, derived a solar irradiance reduction of about 0.65% below the 1980 level during the Maunder Minimum. Forcing an one-dimensional ocean-climate model (Hoffert et al., 1980) with his irradiance variations and a reconstructed historical increase in anthropogenic greenhouse gas forcing, Reid simulated, as expected, a increase in temperature from the time of the Maunder Minimum to 1980 of the order of 1 °C; the change in temperature due to solar forcing alone accounting for about 0.45 °C between 1980 and the coldest year of 1697. Nevertheless, it must be noted that such a irradiance reduction of 0.65% leads to a radiative flux reduction at the top of the atmosphere of about 1.55 Wm^{-2} which is substantially larger than previous independent estimations accounting for about 0.7 Wm^{-2} (Lean et al., 1992), 0.9 Wm^{-2} (Hoyt and Schatten, 1993), and 1 Wm^{-2} by Nesme-Ribes et al. (1993) for this period.

Here, we would like to question two of Reid's assumptions. First, Reid only considers solar forcing and anthropogenic greenhouse-gas forcing in his work while a number of recent statistical and numerical studies have shown that the inclusion of the anthropogenic sulfate aerosols forcings leads to a better agreement between the simulated and observed temperature changes (e.g., Kaufmann and Stern, 1997; Houghton et al., 1996). Secondly, we have shown above that his model simulated a

global temperature change of about 0.45 K in response to about 1.55 Wm^{-2}, which suggests therefore a climate model sensitivity to the solar forcing in the range of 3.4 Wm^{-2} K^{-1} (or little less, taking into a ccount thermal inertia). Such a climate model sensitivity was also found (about 3 Wm^{-2} K^{-1}) when Crowley and Kim (1996) forced their EBM with the 0.9 Wm^{-2} radiative forcing from the Hoyt and Schatten (1993) total irradiance reconstruction. By contrast, investigating with a fully coupled state-of-the art GCM (O-AGCM) the effect of variations in the solar constant on the terrestrial climate, Cubasch et al. (1997) simulated a temperature change of 0.5 K in response to the Hoyt and Schatten (1993) reconstruction, which is approximately the expected value for a model with an equilibrium sensitivity of about 1.7 Wm^{-2} K^{-1} (the albedo in this model being larger, 36%, than the usual best guess value of 30%).

Since the amplitude of the climate response is affected by the model estimate of climate sensitivity, we can reasonably hypothesize that if the O-AGCM had been forced with the changes in solar irradiance as reconstructed by Reid (1997), the model response would be close to the temperature drop of about 1 °C from modern values during the Maunder Minimum. This would therefore mean (if its climate sensitivity is correct) that the major part of the observed global warming over the last 150 years is due to the solar forcing. However, as Reid concedes, smaller estimates for the Sun's variability agree more with recent work by solar physics experts. We have therefore focused our investigations on potential changes in solar radiation of 0.05 to 0.30% on centennial time scales.

The three time series of estimated solar irradiance changes used in this study are presented on Figure 1a. Figure 1b allows us to compare these three reconstructions with the recorded Northern Hemisphere temperature variations since 1610. The first and the simplest reconstruction, Sc.WH, is based on the Willson and Hudson (1988) parametrization. They correlated, over the time period 1980–1986, the ACRIM (Active Cavity Radiometer Irradiance Monitor) daily mean data of total solar irradiance with the Wolf sunspot number, R_z, and suggested the following relationship:

$$S = 1366.82 + 7.71 \times 10^{-3} R_z\,, \tag{1}$$

where S is in Wm^{-2}. This parameterization was used here and assumed to be valid over the last centuries. The Wolf sunspot number data (1700–1992) were supplied by the Sunspot Index Data Center of Uccle (Belgium).

The second reconstruction, Sc.LN, (Lean et al., 1995) is based on two separate components; an 11-year cycle or Schwabe cycle plus a slowly varying background. The first is based on an empirical analysis of the relationship between sunspot number (as a surrogate for faculae) and directly observed total irradiance (corrected for sunspot blocking) coupled with historical measurements of sunspot number. Long term changes in solar total irradiance reconstructed with the Schwabe cycle as the only cause of variability are of the order of 0.05%. The background component is a longer term variability component needed to account for the irradiance

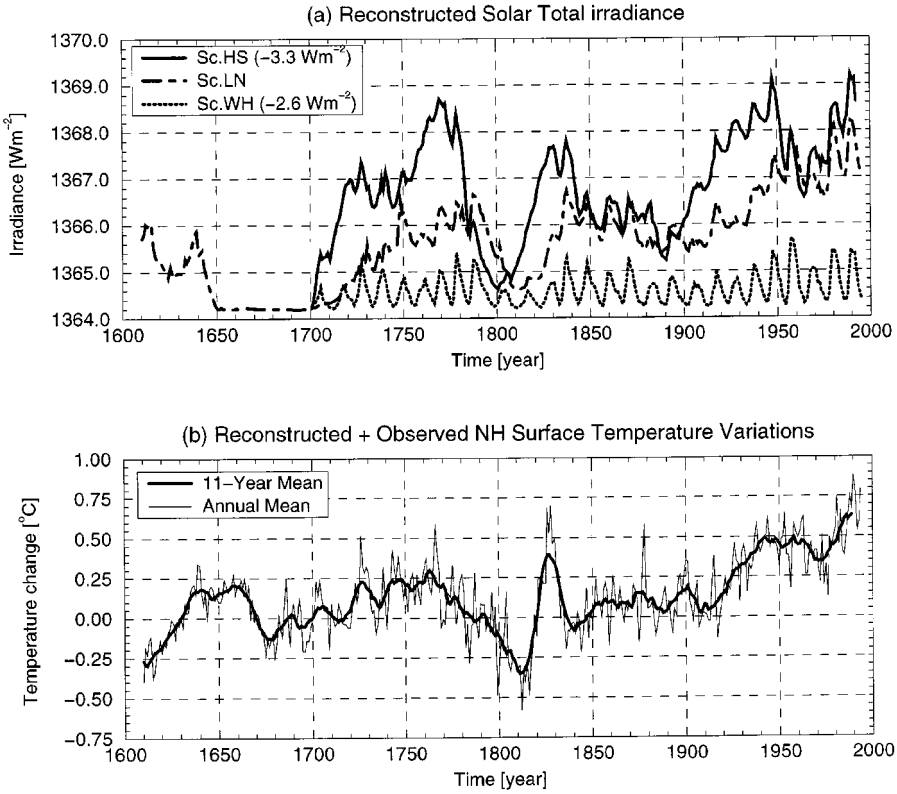

Figure 1. Comparison between the three reconstructed solar total irradiance variations used in this study (a) and the recorded Northern Hemisphere temperature variation from 1610 to 1992 (b). The three time series have been scaled at the Lean et al. (1995) irradiance value in 1700. The annual mean Northern Hemisphere temperature variations are taken from Groveman and Landsberg (1979) for 1700 to 1879 and from Jones (1988 updated) for 1880 to 1992.

reduction estimated independently for the Maunder Minimum (1645–1715) from observations of Sun-like stars. The background variations have been fitted to the average amplitude of the group sunspot number in each Schwabe cycle. Lean et al. (1995) scaled this longer term component to cause an increase of 0.19% in solar total irradiance from the Maunder Minimum to the present. Therefore, by including both components, the overall variability from the Maunder Minimum to the present-day mean is constrained to agree with a solar total irradiance change of 0.24% as estimated by Lean et al. (1992).

A different approach to inferring variability in solar output was presented by Hoyt and Schatten (1993), who consider five different solar indices (the fraction of penumbral spots, the length of the solar cycle, the changes in the equatorial solar rotation rate, the decay rate of the solar cycle, and the mean level of solar activity) which are considered as a measure of secular changes in solar convective energy transport and thus of solar irradiance changes.

TABLE I

Correlation coefficients between the solar irradiance reconstructions (Sc.HS = Hoyt and Schatten (1993), Sc.LN = Lean et al. (1995), Sc.WH = the Willson and Hudson (1988) parametrization) and the recorded annual mean Northern Hemisphere temperature variations from 1700 to 1992

Solar forcing	Correlation
Sc.HS	0.62
Sc.LN	0.57
Sc.WH	0.28

The long term change in solar total irradiance reconstructed with the Willson and Hudson parametrization (1988) which considers the Schwabe cycle as the sole cause of variability are of the order of 0.05%. The maximum variation over the investigated time period is about 1.5 Wm^{-2} ($\sim$0.1%) and occurs during solar cycle 19 (around the year 1957). By contrast, the magnitude of the 1700–1992 change is slightly larger for Sc.HS than estimated in Sc.LN (0.30% vs. 0.24%). The noticeable differences which appears between these three reconstructions (see Figure 1a) reflect the large uncertainties in reconstructing historical solar irradiances from a limited solar monitoring database, with only rudimentary knowledge of the pertinent physical processes (Lean et al., 1995). For example, the timing of changes between the Sc.HS and Sc.LN reconstructions are out of phase with each other with variations occurring approximately 20 years earlier in the Sc.HS time series. This lag results from a long term variability component based on the length of the Schwabe cycle in the Sc.HS rather than average amplitude as it is done in the Sc.LN reconstruction.

If the solar irradiance is varying, it can be expected to affect the temperature of the Earth. The comparison of Northern Hemisphere temperature variations since 1700 and solar forcing is presented Table I. The calculated correlations vary from 0.3 to 0.6, thereby suggesting that solar variability could account for 8 to 38% of the variance in the Northern surface temperature changes over this time period. However, the connection between insolation and surface temperature is complicated by the likely role of feedbacks in the climate system. Therefore, it is useful to compare the surface temperature simulated by a climate model in response to these solar forcing changes and the reconstructed and observed temperature variations during the same period.

3. Model Description and Experimental Setup

3.1. MODEL DESCRIPTION

All simulations were carried out using our two-dimensional (latitude, altitude) sector averaged climate model (Gallée et al., 1991) extended to both hemispheres as used in Bertrand et al. (1999). It has a latitudinal resolution of 5°. In each latitudinal belt the surface is divided into oceanic or continental surface types, each of which interacts separately with the subsurface and the atmosphere. The oceanic surfaces are ice-free ocean and sea ice, while the continental surfaces are snow-covered, snow-free land and ice covered.

The atmospheric dynamics consists of the classical two-level quasi-geostrophic system written in pressure coordinates and zonally averaged. It includes a parameterisation of the meridional transport of quasi-geostrophic potential vorticity and a parameterisation of the Hadley meridional sensible heat transport. Precipitation, vertical radiative (solar and infrared) and turbulent (sensible and latent) heat fluxes, and surface friction are also represented and provide a coupling between the atmosphere and the surface. Unlike the atmospheric dynamics, the radiative transfer computation accounts for 10–15 layers, the exact number depending on the surface pressure over each surface type. The solar radiation scheme is an improved version of the code described by Fouquart and Bonnel (1980). The long-wave radiation computations are based on Morcrette (1984) wideband formulation of the radiative transfer equation. The seasonal cycle of the incoming solar radiation at the top of the atmosphere is computed as a function of the latitude, the semi-major axis of the ecliptic, its eccentricity, its obliquity and the longitude of the perihelion, following Berger (1978). Separate energy balances are calculated over the various surface types at each latitude. At the top of the model, solar and IR fluxes contribute to the net energy flux available to the system. The heating of the atmosphere due to the vertical heat fluxes is the weighted average of the convergence of these fluxes above each kind of surface. The other surface and subsurface parameters and processes which are represented are the surface albedo of each surface type, the oceanic heat transport, the oceanic mixed-layer dynamics, the snow and sea-ice budget, and the water availability at the surface.

The upper-ocean is represented by an integral mixed-layer model in which meridional convergence of heat is given by a diffusive law. In order to perform our transient simulations, the model is coupled to a diffusive ocean in which the uptake of heat perturbations by the deep ocean was approximated by a diffusion process as in Smits et al. (1993). The model time step is 3 days, except for the mixed-layer and sea ice computations, for which it is 1 day.

3.2. EXPERIMENTAL SETUP

The experiment discussed in the present study consists of two parts. Starting from present climate initial conditions, the model was first run until an equilibrium seasonal cycle was established. The equilibrium was supposed to be achieved when the annual global mean radiative balance at the top of the atmosphere becomes less than 0.01 Wm^{-2}. This was reached after 100 years of integration. During the first 100 years of simulation (equilibrium run) the solar constant value as well as the orbital element were kept fixed to their corresponding values in 1610 in the case of Sc.LN reconstruction and 1700 for the two other time series. No exchange of heat at the base of the superficial ocean was allowed at this stage of the simulation. Using this solution as new initial conditions, the model was then integrated from 1610 (1700) to now. In this second part of the simulation (transient run), we mimic, as a diffusion process, the flux of temperature anomalies from the superficial ocean into the deep ocean; and the solar forcing is allowed to vary. Since our simplified model exhibits no internal variability when its equilibrium state is reached, we can obtain a quantitative assessment of the time-dependent response to any change in the solar forcing (changes in the Earth's orbital elements as well as changes in solar activity).

Although we have seen above (introduction) that solar studies indicate that UV variability is proportionally larger than variability in the visible band, our calculation assumed a uniform reduction in insolation forcing. Our justification for this lies in the calculated changes in the 200–300 nm UV band which represent only 7% of the total estimated irradiance change (Lean et al., 1995). Then it seems reasonable, at the present stage of knowledge, that dynamical processes generated by UV modulation of the ozone layer are likely to be important as cause of climate variations on a regional scale, but in a following and possibly amplifying role, rather than in a leading role.

4. Results and Discussion

4.1. ORBITAL FORCING

A first experiment was performed to quantify the influence of the Earth's orbital elements on the time evolution of climate at the secular time scale. In this experiment, the Earth's orbital elements were permitted to vary according to Berger (1978) while the solar total irradiance was kept constant to its 1700 value (1367.52 Wm^{-2}) as given by Hoyt and Schatten (1993). The changes in these elements generate a decrease in the hemispheric annual mean insolation received at the top of the atmosphere of only 0.0007 Wm^{-2} between 1700 and 1992. This very small change comes from the decrease in eccentricity, e, of 0.7% between 1700 and 1992. Indeed, the main parameter affecting the annual and hemispherical mean

insolation, WW, is the eccentricity of the elliptical orbit of the Earth around the Sun.

$$WW = \frac{S}{4} \cdot \frac{1}{\sqrt{1-e^2}}, \tag{2}$$

where S is the solar energy flux measured at the distance a (the semimajor axis of the Earth orbit around the Sun) from the Sun as reconstructed, for example, by Willson and Hudson (1988), Hoyt and Schatten (1993), and Lean et al. (1995); a being considered as invariable in time (Berger, 1977). S is related to S_o, the 'solar constant' by

$$S = S_o(\frac{r_m}{a})^2, \tag{3}$$

with r_m the mean distance from the Earth to the Sun; distance which varies as a function of e.

The behaviour can be quite different for a particular month as illustrated Figure 2. Indeed, as shown in Figure 2b, from 1700 to 1992 the Northern (Southern) Hemispheric mean incident solar radiation has increased by 1.17 (0.98) Wm^{-2} in April (March) and decreased by 1.22 (1.31) Wm^{-2} in September (November). These larger variations come from the inclusion of the solar declination, δ, and the normalised distance from the Earth to the Sun, ρ, in the computation of the instantaneous hemispherical mean insolation, $WW^\star$.

$$WW^\star = S \cdot \frac{1}{\rho^2} \cdot \frac{1}{4}(1 \pm \sin\delta). \tag{4}$$

Another difference between the two hemispheres appears when we compare the number of months for which the hemispheric mean incident solar radiation is enhanced. While six months of increased incident solar radiation are followed by six months of decreasing incident solar radiation in the Northern Hemisphere, only four months of decreasing incident solar radiation appear in the Southern Hemisphere (Figure 2b). This difference introduced by the solar declination, δ, leads to an opposite annual and hemispheric response to the orbital forcing. Figure 2d shows that these insolation variations induce in the model a hemispheric annual mean surface cooling of 0.006 °C in the Northern Hemisphere while a warming of 0.004 °C is simulated in the Southern Hemisphere at the end of our simulation.

This opposite hemispherical temperature response to the variations in the insolation received at the top of the atmosphere results from the associated modification in sea-ice and snow areas. As shown in Figure 3a, the increase in ice and snow field areas in the Northern Hemisphere is related to the long-term decrease in insolation during the melting period while the decrease occurs during the months of maximum extension. The area increase being larger than the decrease, the averaged increase is about 0.15% for sea-ice area and about 0.12% for the snow field area increase. In the Southern Hemisphere (Figure 3b), the positive insolation anomaly

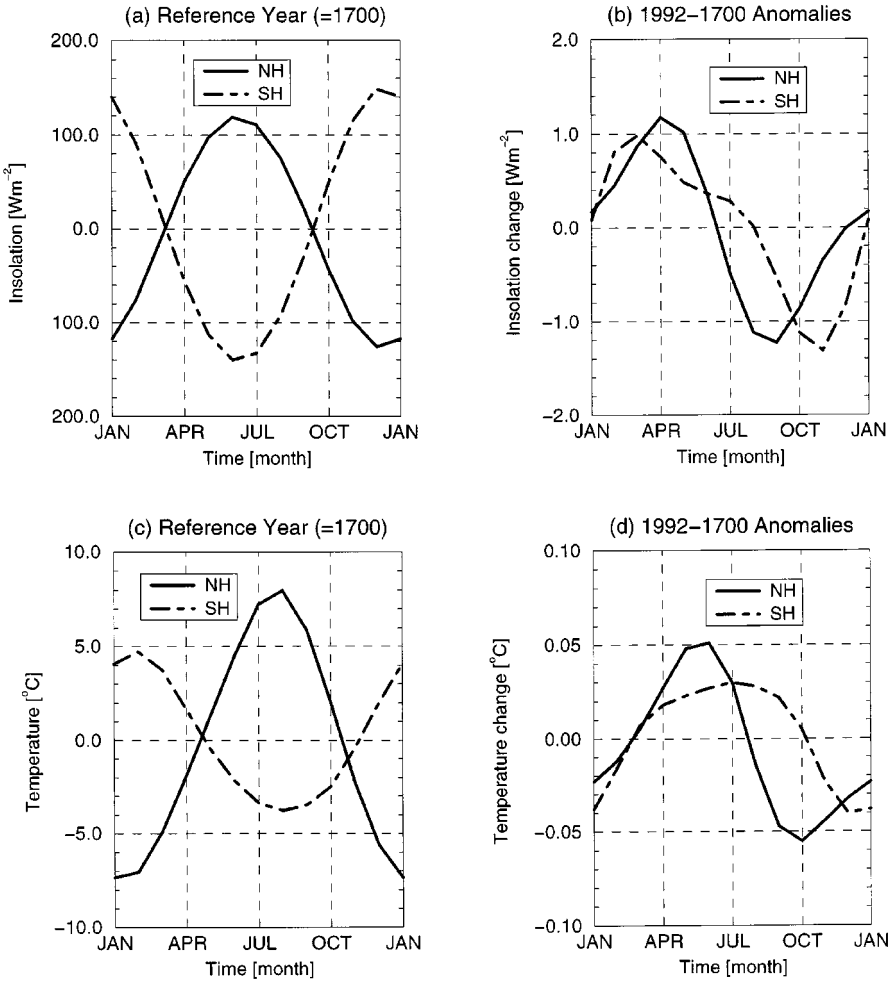

Figure 2. Variations in insolation received at the top of the atmosphere and in surface temperature since 1700 due to the changes in the Earth's orbital elements. (a) presents the seasonal cycle of the insolation variation relative to the annual mean value in each hemisphere for the year 1700 while (b) exhibits the montly mean insolation anomalies due to the Earth's orbital elements variations from 1700 to 1992. The Earth surface temperature seasonal cycle are shown (c) relative to the annual mean value in each hemisphere for the year 1700 and the temperature anomalies introduced in response to the Earth's orbital elements from 1700 to 1992 are given in monthly mean (d).

during the months of minimum ice and snow area as well as during the months of ice and snow formation leads to a progressive reduction in ice and snow field areas. Indeed, due to the large seasonal cycle of ice area and the low snow area in this hemisphere, the long term decrease in insolation during the time period from October to January is not sufficient to balance, in annual mean, the ice and snow

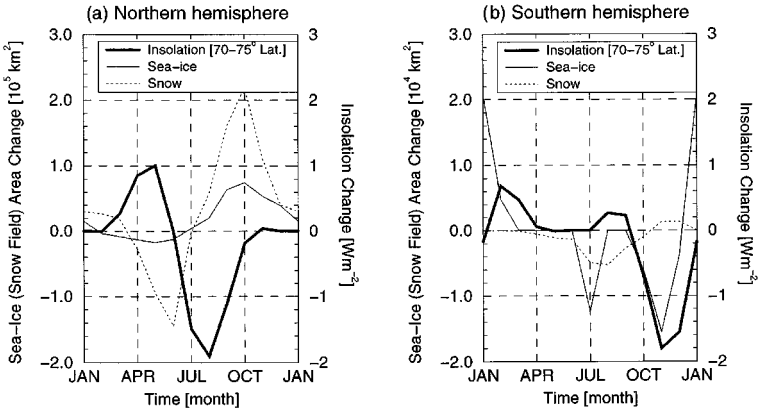

Figure 3. Comparison between the monthly mean sea-ice and snow area anomalies with the insolation anomalies in Wm^{-2} at the 70–75° latitudinal band in response to the orbital forcing from 1700 to 1992 in each hemisphere. (a) Northern Hemisphere. (b) Southern Hemisphere.

reduction. At the end of our simulation the annual mean decrease in sea-ice area is 0.06% while the snow field area decreases by 0.57%.

4.2. TOTAL SOLAR IRRADIANCE FORCING

A second experiment was carried out in which the Earth's orbital elements were kept fixed to their equilibrium run values, while the total solar irradiance was allowed to vary according to the three reconstructions discussed in Section 2. Figure 4 presents the time evolution of the annual global (Figure 4a) and hemispheric (Figures 4b and 4c) mean surface temperature simulated by the model. Despite the apparently good agreement between the shape of the curves of the Sc.LN and Sc.HS reconstructed irradiances and that of Northern Hemisphere temperature variations as presented in Figure 1 and Table I, the simulated air surface temperature response to these reconstructions are clearly insufficient to reproduce the temperature variations over the last three centuries. The range of maximum temperature variation simulated over this time period is between 0.07 to 0.37 °C in global mean. This response, which is slightly larger than the 0.3 °C obtained by Crowley and Kim (1996) and a little bit lower than the 0.5 °C of Cubasch et al. (1997), is approximately the expected value for a model with an equilibrium sensitivity of about 1.8 Wm^{-2} K^{-1} (the model albedo being slightly larger than 32%).

The simulated Northern Hemispheres surface temperatures account only for 18 to 37% of the recorded Northern Hemisphere temperature variance over the time period 1700–1992 (see Table II). It will be surprising for the reader that a larger correlation is found between the surface temperature response to the Sc.WH reconstruction and the observations than directly between the Sc.WH time series and the observations. The reason comes from the spatial distribution of the points

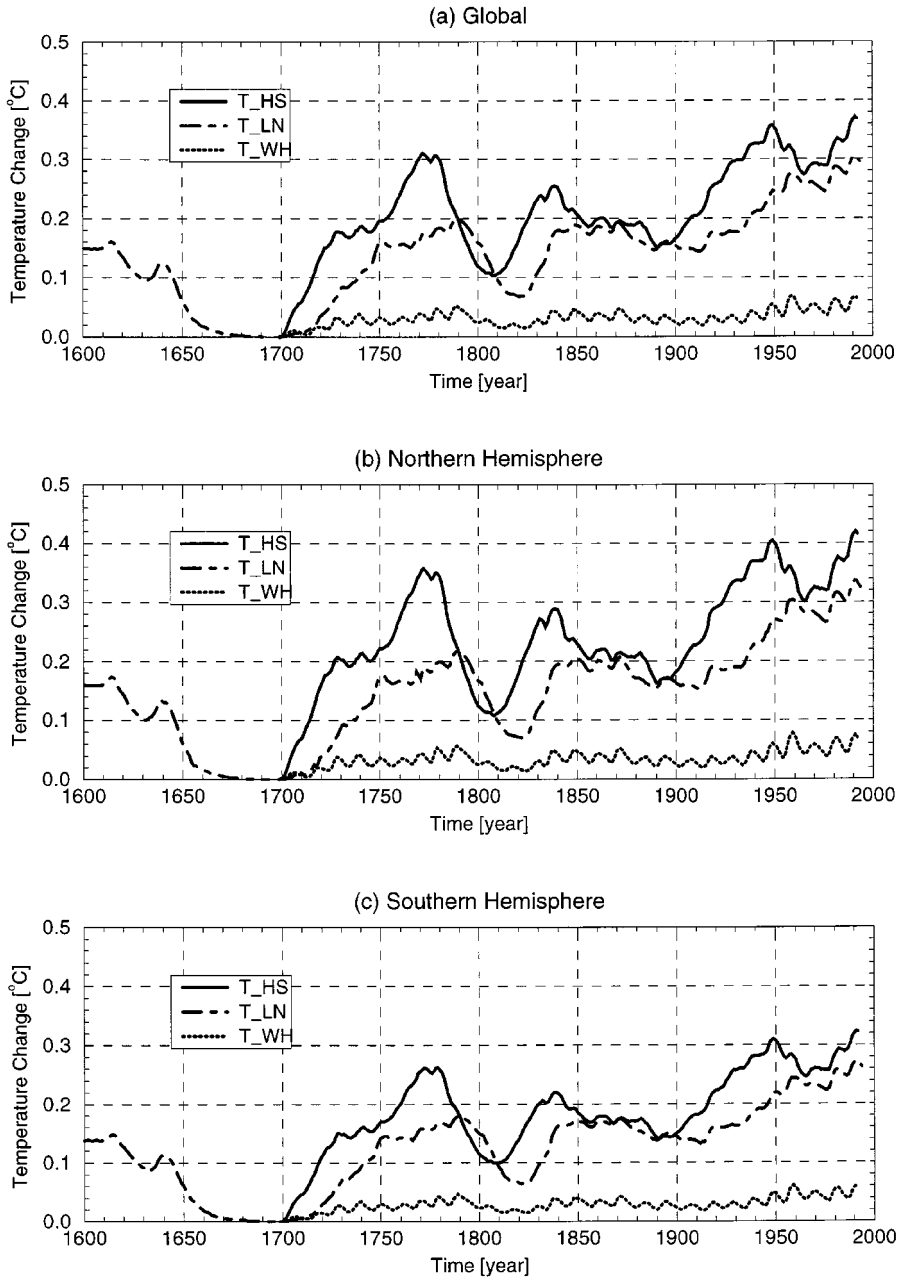

Figure 4. Comparison between the time evolution (relative to the 1700 values) of the annual global (a) and hemispheric mean (b: Northern Hemisphere and c: Southern Hemisphere) surface temperature response to the three investigated solar forcings.

TABLE II

Percentage of the observed temperature variance over the time period 1854–1992 explained from the model response to the Hoyt and Schatten (1993), Sc.HS, Lean et al. (1995), Sc.LN, and the Willson and Hudson (1988) parametrization, Sc.WH, solar total irradiance reconstructions

Solar forcing	Explained variance (%)		
	T_{Global}	T_{NH}	T_{SH}
Sc.HS	60.0	56.0 (37.0)	52.0
Sc.LN	63.0	54.0 (23.0)	60.0
Sc.WH	38.0	32.0 (18.0)	38.0

Values in parentheses beside the T_{NH} variance value is the explained variance over the time period 1700–1992.

around the regression line which is so spread in these two cases that the relevance of such correlations can be clearly questioned.

The different amounts and distributions of land and ocean between the two hemispheres lead to a larger temperature response to the solar forcing in the Northern Hemisphere (0.08–0.42 °C) than in the Southern Hemisphere (0.06–0.32 °C) as shown in Figures 4b and 4c. An important feature of this figure is that while the simulated temperatures seem to reproduce the major trends of the recorded one's, the amplitude are not. Volcanic forcing could have played in connection with decreasing stages of the Gleissberg cycle in the solar forcing to amplify some cooling periods. Nevertheless, the combination of intense volcanic activity and reduced solar activity seems to be inadequate to explain the low temperatures of the Maunder Minimum Period. As an example, Zielinski (1995) showed that the late 17th century was a period of relatively normal stratospheric sulfate loading, and was followed by more frequent volcanic activity during the 19th and 20th centuries.

Figures 5a and 5b display the time evolution of the annual mean total sea-ice area simulated in each hemisphere by the model. Due to a very quiet Sun at the start of the integrations, the ice area is maximum during the Maunder Minimum (1645–1715) and exhibits a decreasing trend after this period. Some periods of sea-ice recovery appear in connection with the decreasing stages of the Gleissberg cycle in the solar forcing around 1800, 1890 and 1970. The continental snow area (not shown) exhibits a similar behaviour.

The evolution of the annual mean latitudinal distribution in zonal and sectorial average of the simulated air surface temperature response to the solar forcing as reconstructed by Hoyt and Schatten (1993) is given in Figure 6. Only the response to this forcing is shown because similar patterns are found in response to the Sc.LN and Sc.WH reconstructions. It is worth pointing out that the time series of the latitudinal distribution of the modelled surface temperature change indicates that

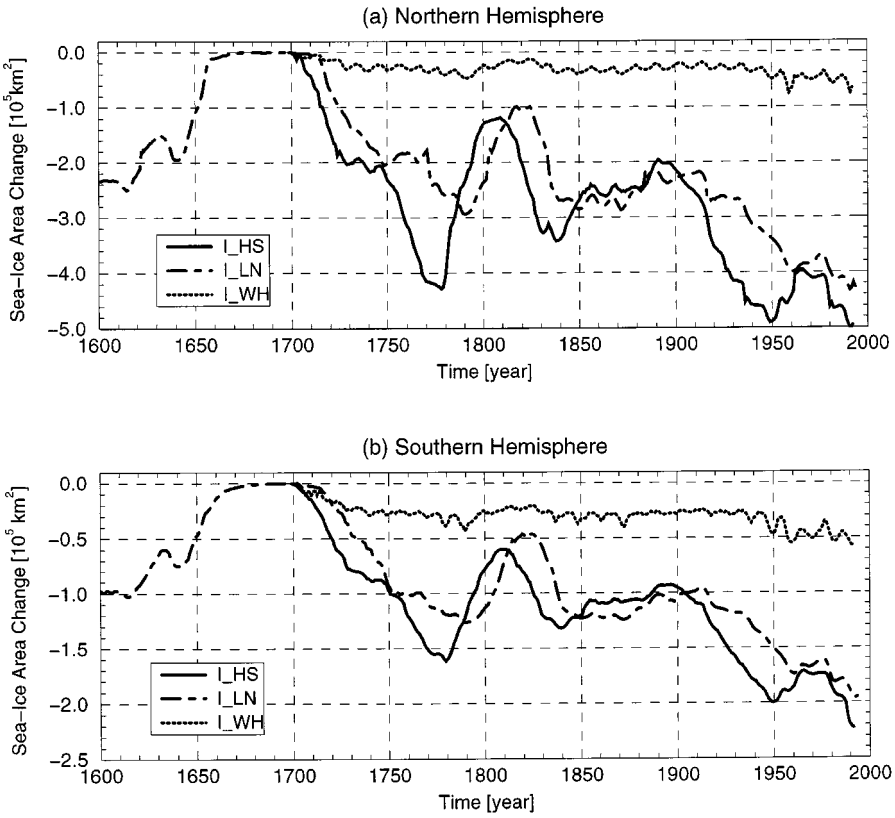

Figure 5. Comparison between the time evolution of the annual mean hemispheric (a: Northern Hemisphere and b: Southern Hemisphere) total sea-ice area (relative to the 1700 values) simulated by the model in response to the three investigated solar forcings.

the largest temperature variations are located at latitudes higher than 70° during both warming and cooling periods. This behaviour is related to the amplification of the climate response due to the ice (Figure 6b) and to a lesser extent to the snow (Figure 6c) albedo-temperature feedback. However, due to the larger seasonal cycle of sea-ice in the Southern Hemisphere and low ice area in summer, the major air surface temperature variations appear in the Northern Hemisphere. The larger air temperature variation simulated above the Northern ice sheet compared to the Southern ice sheet (Figure 6d) results from the influence of these more important sea-ice temperature variations. The discontinuity which appears in zonal (Figure 6a) and oceanic (Figure 6b) average mean surface temperature response around 60° S corresponds to the maximal sea-ice extent in this hemisphere. Such a discontinuity is not simulated in the Northern Hemisphere due to the lower thermal inertia of continents which allows a smoother transition between the high and middle latitudinal temperature response (Figure 6c).

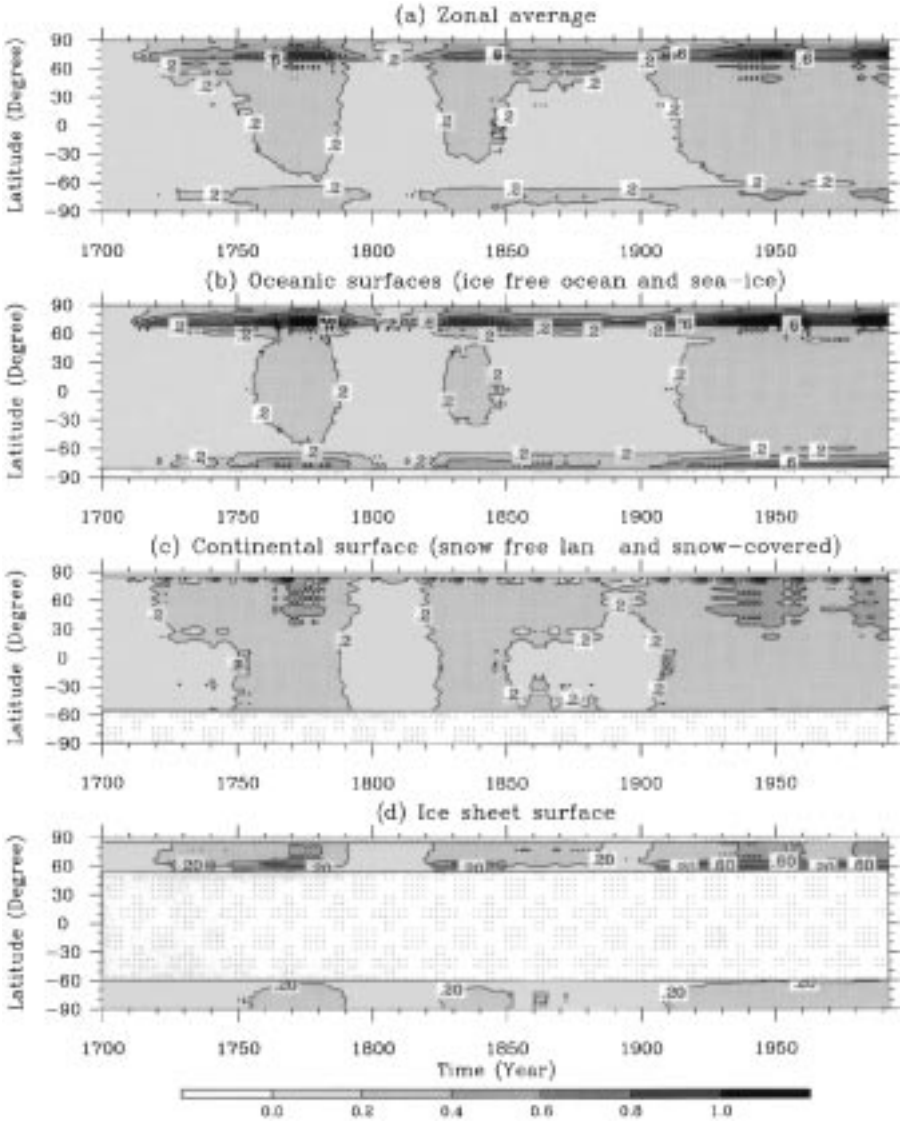

Figure 6. Time evolution of the annual mean latitudinal distribution of the simulated surface temperature response (in °C) to the Hoyt and Schatten (1993) total solar irradiance reconstruction, relative to the equilibrium state. (a) sector averaged, (b) oceanic surfaces (ice-free ocean and sea ice), (c) continental surfaces (snow-free land and snow-covered) and (d) ice covered continents.

All these model responses to the solar reconstructions (Figures 4 to 6) clearly indicate that the dominant response to the solar forcing is at the scale of Gleissberg cycle (with peak-to-trough changes largely depending on the solar reconstruction). The influence of the 11-year solar cycle forcing is much less visible excepted for the particular reconstruction of Willson and Hudson (1988) and in the simulated

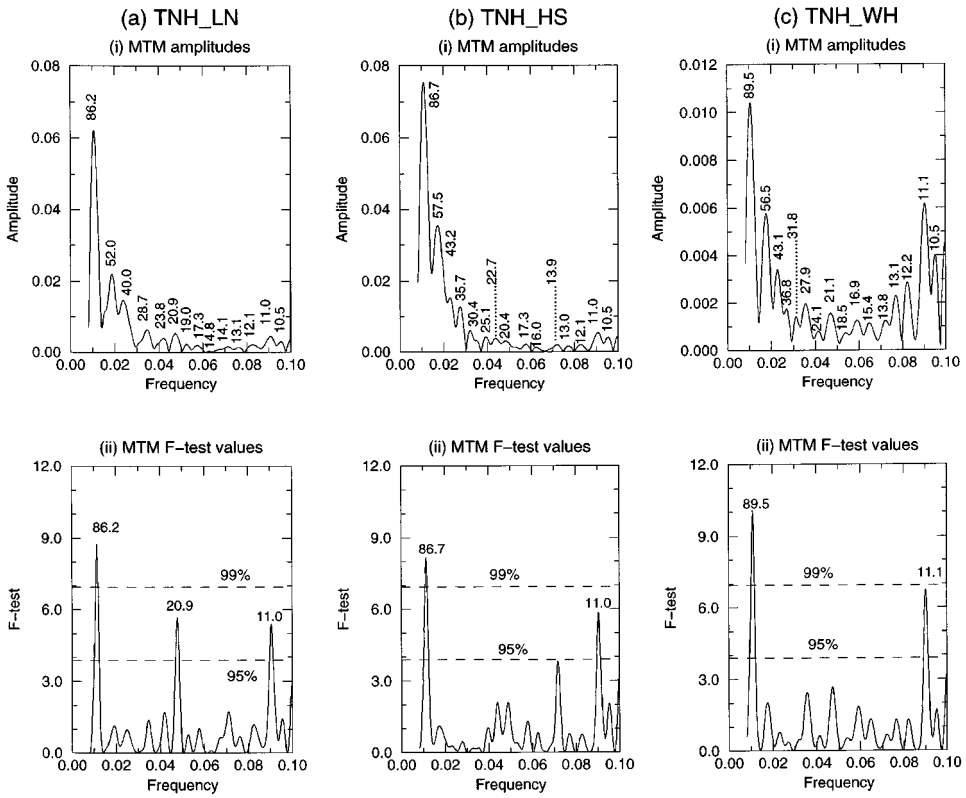

Figure 7. Multi-taper Thomson (MTM) spectral analysis of the 293 years long (1700–1992) annual mean Northern Hemisphere surface temperature simulated by the model in response to the solar forcing as reconstructed by (a) Lean et al. (1995), TNH_LN, (b) Hoyt and Schatten (1993), TNH_HS, and (c) by the Willson and Hudson (1988) parametrization, TNH_WH. The first panels (i) present for each cases, the amplitudes of the detected cycles and their associated periods. The lower panels (ii) represent the corresponding F-test values. The periods significant at the 95% level are quoted.

temperature variations over Northern Hemisphere snow areas (see Figure 6c). This is confirmed by applying the multi-taper Thomson spectral analysis method (MTM) (Thomson, 1982, 1990) to the time series of the annual mean Northern Hemisphere surface temperature simulated by the model from 1700 to 1992 (see Figure 7).

The purpose of this non-parametric spectral method is to compute a set of independent and significant estimates of the power spectrum, in order to obtain a more reliable estimate than with single-taper methods given a finite time series. MTM analysis is based on the property that it minimizes leakage outside a chosen spectral bandwith and thus produces an optimal set of band-limited spectral estimates in the Fourier transform sense. Moreover, MTM provides a high spectral resolution together with a signal-to-noise ratio F-test to estimate the validity of the location, amplitude and statistical confidence of each peak in the spectrum (Park et al., 1987;

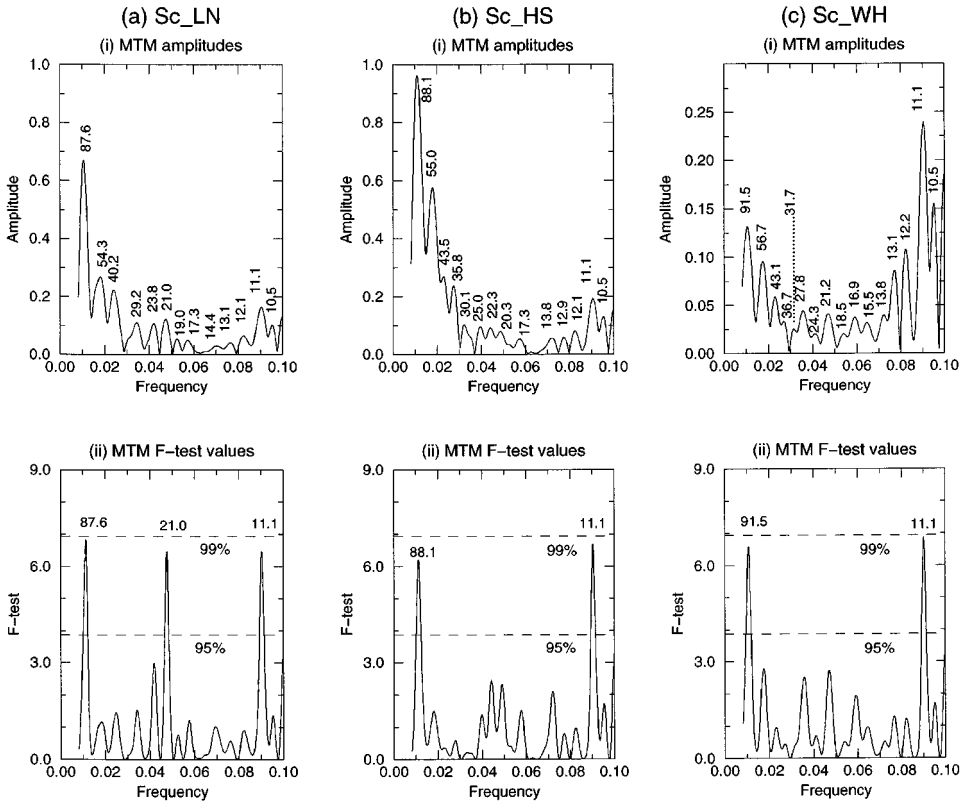

Figure 8. Multi-taper Thomson (MTM) spectral analysis of the 293 years long (1700–1992) total solar irradiance reconstruction as given by (a) Lean et al. (1995), Sc_LN, (b) Hoyt and Schatten (1993), Sc_HS, and (c) by the Willson and Hudson (1988) parametrization, Sc_WH. The first panels (i) present for each cases, the amplitudes of the detected cycles and their associated periods. The lower panels (ii) represent the corresponding F-test values. The periods significant at the 95% level are quoted.

Thomson, 1990). The method may therefore separate the deterministic component (e.g., the peak corresponding to each sine wave) from the non-deterministic part of the process. As the confidence level of the F-test is independent of the amplitude of each peak, the method is able to detect a low-amplitude period with a high degree of statistical significance or to reject a high-amplitude period if it fails the F-test. It turns out in practise that this test is robust to the white noise assumption and still gives reasonably good results with colored noise. MTM analysis is also able to extract, from very short time series, significant low-frequency components with periods close to the series length.

Figure 8 provides the comparison between the spectra of the different solar insolation curves. What is interesting to note on this figure is that while the modeled temperature responses present frequencies similar to those detected as significant above the 95% level by the MTM F-test in the corresponding solar irradiance

curves (around 88 and 11 years, and at the 22 years Hale solar cycle in the case of the Sc.LN reconstruction), none of these extracted frequencies are found in the recorded temperature time series (see Figure 9). Note that the little shift which appears at low frequencies between irradiance spectra (Figure 8) and simulated temperature spectra (Figure 7) is probably due to a signal distorsion at low frequencies. It must be noted, however, that by reducing the confidence level from 95% to 88%, a 96-year signal is found in the reconstructed temperature (Figure 9b). This seems to indicate that the detected 96-year signal is not a straight signal from solar forcing but rather the combination of a solar signal with other natural (internal or external) periodic signal(s). Indeed, in view of the detected periodic signals on the simulated temperatures, we can reasonably assume that if this signal was a pure solar signal, it should have been found at the 95% confidence level and its periodicity should have been similar to that found in the irradiance curve.

Figure 9 also indicates that the recorded temperature exhibits significant periodicities around 17, 12 and 10 years (already found at the 95% confidence level). Once again, none of these periods is detected as significant above the 95% level by the MTM F-test in the simulated and irradiance time series. Both simulated temperature and irradiance curves present a periodic signal around 11 years. As already mentioned, this Schwabe cycle signal is easily detected in the latitudinal band 85–80° N in Figure 6c and illustrates well the strong sensitivity of the small portion of land present in these high latitudes due to the snow albedo temperature feedback. Such a result could indicate that the eleven-year period which is frequently found in climate data might be related to oscillations in the atmosphere or oceans, internal to the climate system. A combination of, for example, biannual and quasi-biennial oscillations could induce 10- to 12-year periodicities and hence lead to correlations similar to those observed, but unrelated to solar forcing (Dunkerton and Baldwin, 1992). In addition, internal variability of the climate system, or other mechanisms such as changes in ocean circulation, could also lead to 10- to 12-year oscillations over short records (Houghton et al., 1994). An alternative to this could be that these periodicities come from the combination of the purely radiative solar signal with a 'dynamical' solar signal resulting from the Sun modulation of the ozone layer as discussed in the introduction. Due to the relative simplicity of our climate model the possible climatic impacts of UV irradiance variations have been neglected and need therefore further investigations with more sophisticated climate models in order to highlight such a possibility.

Finally, while solar activity has risen systematically through the past 100 years, none of the three solar irradiance reconstructions is able to introduce a model response comparable to the observed global 20th century warming of 0.53 ± 0.07 °C (Jones, 1992). Indeed, if the Willson and Hudson (1988) is correct, then only 7.5% of the observed global warming and 38% of the variability in global mean temperature over this time period could be attributed to solar variability. If on the other hand, the Hoyt and Schatten (1993) reconstruction is correct, then 33.6% and 60% of these values, respectively, could be so explained (see Table II). Nevertheless,

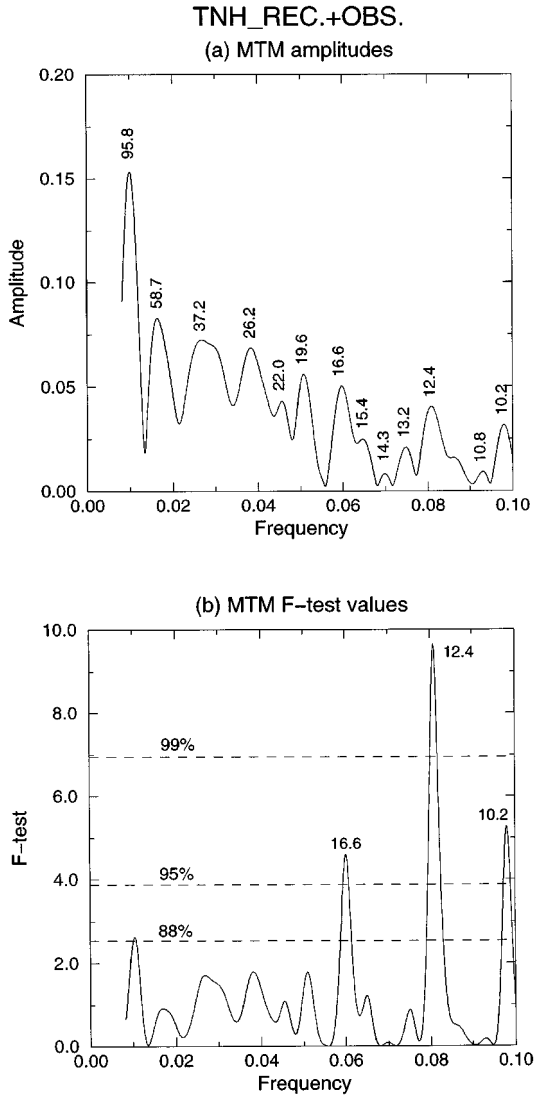

Figure 9. Multi-taper Thomson (MTM) spectral analysis of the 293 years long (1700–1992) of the recorded annual mean Northern Hemisphere temperature variations taken from Groveman and Landsberg (1979) for 1700 to 1879 and from Jones (1988 updated) for 1880 to 1992. Panel (a) presents the amplitudes of the detected cycles and their associated periods. Panel (b) represents the corresponding F-test values. The periods significant at the 95% level are quoted.

the greatest care must be taken in the interpretation of the variances quoted above. Indeed, by contrast to a purely statistical model, it is not at all certain that all the conditions needed for the regression are met here.

5. Conclusion

A two-dimensional sector averaged climate model has been used to determine the possible relative importance of the solar and astronomical forcings on the climate of the last three centuries. It has been shown, in accordance with the previous modelling study of Smits et al. (1993), that the annual and hemispheric mean radiative forcing due to orbital changes are negligible on the century time scale. However, for a particular month the behaviour can be quite different. The combination of eight months of increasing insolation with a well-marked seasonal cycle of sea-ice in the Southern Hemisphere leads to a net annual mean warming while a net cooling is simulated in the Northern Hemisphere. These temperature change are however negligible at the secular time scale.

The good apparent correlation between the reconstructed solar total irradiance changes based on solar models of Hoyt and Schatten (1993) as well as from Lean et al. (1995) and the recorded temperature variations over the last three centuries seems however insufficient to explain the observed global warming by the sole variations in the Sun's radiant energy output. Indeed, while solar activity has risen systematically through the past 100 years, as recorded in the number of sunspots, none of the three solar total irradiance reconstructions investigated here, present irradiance changes able to induce a climate model response similar to the observed global 20th century warming. The modeled global warming over the last 100 years of 0.22 °C in the higher case and of 0.045 °C in the lower case represents only 33.6% and 7.5% of the observed change (0.53 ± 0.07 °C) (Jones, 1992). Over a still longer time period, the model presents a global cooling of 0.31 °C for the Maunder Minimum when forced by the 0.24% irradiance reduction included in the Lean et al. (1995) reconstruction. The largest Maunder Minimum temperature cooling of 0.37 °C is simulated in response to the Hoyt and Schatten (1993) reconstruction, while the influence of solar irradiance changes due to the photospheric effects encapsulated in the Willson and Hudson (1988) parametrization is limited to Earth surface temperature cooling of 0.07 °C.

Therefore, if satellite measurements confirm the amplitude of irradiance variations associated with the Gleissberg cycle as reconstructed by the solar models Hoyt and Schatten (1993) or Lean et al. (1995), the solar forcing should not be neglected to explain the century-scale climate variations. Indeed, we have shown in accordance with previous work of Cubasch et al. (1997) that the dominant surface temperature response to irradiance change occurs at the centennial-scale Gleissberg cycle. Due to the amplification of the climate response by the snow and ice albedo-temperature feedback, the largest temperature variations are located in the high latitudes during both warming and cooling periods. By contrast, the Schwabe radiation cycle seems too short and its amplitude too small to have any significant influence on the time evolution of climate at the secular time scale. The simulated maximum temperature variation associated with this cycle was about 0.05 °C and occurred around the year 1957. Moreover, MTM spectral analysis seems to point

out that the 10- to 12-year oscillations found in the recorded Northern Hemisphere temperature variations from 1700 to 1992 could be unrelated to solar forcing. Nevertheless, futher investigations including the possible climatic impacts of UV irradiance variations are needed. Indeed, a hypothetized connection between such periodicities and the Sun could be a combination of the purely radiative solar signal with a 'dynamical' solar signal.

Acknowledgements

We thank J. Lean for providing her reconstructed total solar irradiance reconstruction, U. Cubasch for Hoyt and Schatten's solar time series, A. Robock for Groveman and Landsberg's temperature data set, and the Sunspot Index Data Center of Uccle (Belgium) for Wolf sunspot number data. Thanks is also due to Marie-France Loutre for interesting discussion about the Milankovitch forcing and the spectral analysis method. This research was sponsored by the Climate Programme of the Commission of the European Communities under Grants EV5V-CT92-0123 and ENV4-CT95-0102 and supported by the Impulse Programme 'Global Change et développement durable' (Belgian State, Prime Minister's Services, Science Policy Office, Contract CG/DD/242).

References

Berger, A.: 1977, 'Long-Term Variations of the Earth's Orbital Elements', *Celestial Mech.* **15**, 53–74.

Berger, A.: 1978, 'Long-Term Variations of Daily Insolation and Quaternary Climatic Changes', *J. Atmos. Sci.* **35**, 2362–2367.

Berger, A.: 1988, 'Milankovitch Theory and Climate', *Rev. Geophys.* **26**, 624–657.

Bertrand, C., van Ypersele, J.-P., and Berger, A: 1999, 'Volcanic and Solar Impacts on Climate Since 1700', *Clim. Dyn.* **15**, 355–367.

Bradley, R. S. and Jones, P. D.: 1993, '"Little Ice Age" Summer Temperature Variations: Their Nature and Relevance to Recent Global Warming Trends', *Holocene* **3**, 367–376.

Crowley, T. J. and North, G. R.: 1991, *Paleoclimatology*, Oxford University Press, New York, p. 339.

Crowley, T. J. and Kim, K.-Y.: 1996, 'Comparison of Proxy Records of Climate Change and Solar Forcing', *Geophys. Res. Lett.* **23**, 359–362.

Cubasch, U., Voss, R., Hegerl, G. C., Waszkewitz, J., and Crowley, T. J.: 1997, 'Simulation of the Influence of Solar Radiation Variations on the Global Climate with an Ocean-Atmosphere General Circulation Model', *Clim. Dyn.* **13**, 757–767.

Dickinson, R.: 1975, 'Solar Variability in the Lower Atmosphere', *Bull. Amer. Meteorol. Soc.* **56**, 1240–1248.

Dunkerton, T. J. and Baldwin, M. P.: 1992, 'Modes of Interannual Variability in the Stratosphere', *Geophys. Res. Lett.* **19**, 49–52.

Eddy, J. A.: 1976, 'The Maunder Minimum', *Science* **192**, 1189–1202.

Eddy, J. A.: 1988, 'Variability of the Present and Ancient Sun: A Test of Solar Uniformitarianism', in Stephenson, F. R. and Wolfendale, A. (eds.), *Secular Solar and Geomagnetic Variations*, Kluwer Academic Publishers, Dordrecht, pp. 1–23.

Eddy, J. A. and Oeschger, H.: 1993, 'The Role of Solar Output Variations', in Eddy, J. A. and Oeschger, H. (eds.), *Global Changes in the Perspective of the Past*, John Wiley and Sons Ltd, Chichester, pp. 279–294.

Fouquart, Y. and Bonnel, B.: 1980, 'Computations of Solar Heating of the Earth's Atmosphere: A New Parameterization', *Beitr. Phys. Atmosph.* **53**, 35–62.

Friis-Christensen, E. and Lassen, K.: 1991, 'Length of the Solar Cycle: An Indicator of Solar Activity Closely Associated with Climate', *Science* **254**, 698–700.

Gallée, H., van Ypersele, J.-P., Fichefet, Th., Tricot, Ch., and Berger, A.: 1991, 'Simulation of the Last Glacial Cycle by a Coupled, Sectorially Averaged Climate-Ice Sheet Model 1. The Climate Model', *J. Geophys. Res.* **96**, 13,139–13,163.

Groveman, B. S. and Landsberg, H. E.: 1979, 'Simulated Northern Hemisphere Temperature Departures 1579–1880', *Geophys. Res. Lett.* **6**, 767–769.

Haigh, J. D.: 1994, 'The Role of Stratospheric Ozone in Modulating the Solar Radiative Forcing of Climate', *Nature* **370**, 544–546.

Haigh, J. D.: 1996, 'The Impact of Solar Variability on Climate', *Science* **272**, 981–984.

Hickey, J. R., Alton, B. M., Kyle, H. L., and Hoyt, D. V.: 1988, 'Total Solar Irradiance Measurements by ERB/Nimbus 7: A Review of Nine Years', *Space Sci. Rev.* **48**, 321–342.

Hoffert, M. I., Callegari, A. J., and Hsieh, C.-T.: 1980, 'The Role of Deep Sea Heat Storage in the Secular Response to Climate Forcing', *J. Geophys. Res.* **85**, 6667–6679.

Hoffert, M. I., Frei, A., and Narayanan, V. K.: 1988, 'Application of Solar Max ACRIM Data to Analysis of Solar-Driven Climatic Variability on Earth', *Clim. Change* **13**, 267–285.

Houghton, J. T., Meira Filho, L. G., Bruce, L., Hoesung Lee, Callander, B. A., Haites, E., Harris, N., and Maskell, K. (eds.): 1994, *Climate Change 1994: Radiative Forcing of Climate Change and an Evaluation of the IPCC IS92 Emission Scenarios*, Cambridge University Press, Cambridge, p. 339.

Houghton, J. T., Meira Filho, L. G., Callander, B. A., Harris, N., Kattenberg, A., and Maskell, K. (eds.): 1996, *Climate Change 1995: The Science of Climate Change*, Cambridge University Press, Cambridge, p. 572.

Hoyt, D. V. and Schatten, K. H.: 1993, 'A Discussion of Plausible Solar Irradiance Variations, 1700–1992', *J. Geophys. Res.* **98**, 18,895–18,906.

Jones, P. D.: 1988, 'The Influence of ENSO on Global Temperatures', *Climate Monitor* **17** (3), 80–89.

Jones, P. D. and Briffa, K. R.: 1992, 'Global Surface Air Temperature Variations during the Twentieth Century: Part 1, Spatial, Temporal and Seasonal Details', *The Holocene* **2**, 165–179.

Kaufmann, R. K. and Stern, D. I.: 1997, 'Evidence for Human Influence on Climate from Hemispheric Temperature Relations', *Nature* **388**, 39–44.

Kelly, P. M. and Wigley, T. M. L.: 1992, 'Solar Cycle Length, Greenhouse Forcing and Global Climate', *Nature* **360**, 328–330.

Labitzke, K. and van Loon, H.: 1993, 'Some Recent Studies of Probable Connections between Solar and Atmospheric Variability', *Ann. Geophys.* **11**, 1084–1094.

Labitzke, K. and van Loon, H.: 1995, 'Connection Between the Troposphere and Stratosphere on a Decadal Scale', *Tellus* **47A**, 275–286.

Lean, J.: 1989, 'Contribution of Ultraviolet Irradiance Variations to Changes in the Sun's Total Irradiance', *Science* **244**, 197–200.

Lean, J., Skumanich, A., and White, O.: 1992, 'Estimating the Sun's Radiative Output during the Maunder Minimum', *Geophys. Res. Lett.* **19**, 1591–1594.

Lean, J., Beer, J., and Bradley, R.: 1995, 'Reconstruction of Solar Irradiance Since 1600: Implications for Climate Change', *Geophys. Res. Lett.* **22**, 3195–3198.

Morcrette, J. J.: 1984, *Sur la paramétrisation du rayonnement dans les modèles de la circulation générale atmosphérique*, Thèse de Doctorat d'Etat, Univ. des Sci. et Tech. de Lille, Lille, France, p. 373.

Nesme-Ribes, E., Ferreira, E. N., Sadourny, R., Le Treut, H., and Li, Z. X.: 1993, 'Solar Dynamics and its Impact on Solar Irradiance and Terrestrial Climate', *J. Geophys. Res.* **98**, 18923–18935.

Newman, M. J. and Rood, R. T.: 1977, 'Implications of Solar Evolution for Earth's Early Atmosphere', *Science* **198**, 1035–1037.

Park, J., Lindberg, C. R., and Vernon, F. L. I.: 1987, 'Multitaper Spectral Analysis of High-Frequency Seismograms', *J. Geophys. Res.* **92**, 12,675–12,684.

Reid, G. C.: 1991, 'Solar Irradiance Variations and Global Sea Surface Temperature Record', *J. Geophys. Res.* **96**, 2835–2844.

Reid, G. C.: 1997, 'Solar Forcing of Global Climate Change since the Mid-17th Century', *Clim. Change* **37**, 391–405.

Rind, D. and Overpeck, J.: 1993, 'Hypothesized Causes of Decade-to-Century Scale Climate Variability: Climate Model Results', *Quat. Sci. Rev.* **12**, 357–374.

Schlesinger, M. E. and Ramankutty, N.: 1992, 'Implications for Global Warming of Intercycle Solar Irradiance Variations', *Nature* **360**, 330–333.

Schneider, S. H.: 1972, 'Cloudiness as a Global Climate Feedback Mechanism: The Effects on the Radiation Balance and Surface Temperature of Variations in Cloudiness', *J. Atmos. Sci.* **29**, 1413–1422.

Smits, I., Fichefet, Th., Tricot, Ch., and van Ypersele, J.-P.: 1993, 'A Model Study of the Time Evolution of Climate at the Secular Time Scale', *Atmósfera* **6**, 255–272.

Svensmark, H. and Friis-Christensen, E.: 1997, 'Variation of Cosmic Ray Flux and Global Cloud Coverage – a Missing Link in Solar-Climate Relationships', *J. Atmos. Solar-Terr. Phys.* **59**, 1125–1232.

Thomson, D. J.: 1982, 'Spectrum Estimation and Harmonic Analysis', *IEEE Proc.* **70**, 1055–1096.

Thomson, D. J.: 1990, 'Quadratic-Inverse Spectrum Estimates: Applications to Palaeoclimatology', *Phil. Trans. Roy. Soc.* **A332**, 539–597.

van Dorland, R. and van Ulden, A.: 1998, 'Natural and Anthropogenic Variations in the Radiative Balance', in KNMI Symposium Report, *Sun and Climate: The Influence of Variations in Solar Activity on the Earth's Climate*, De Bilt, The Nederlands.

van Ulden, A. and van Dorland, R.: 1998, 'Statistical Relations between Solar Activity Anthropogenic Greenhouse Effect and Global Temperatures from 1856 to 1997', in KNMI Symposium Report, *Sun and Climate: The Influence of Variations in Solar Activity on the Earth's Climate*, De Bilt, The Nederlands.

Wigley, T. M. L. and Kelly, P. M.: 1990, 'Holocene Climatic Change, ^{14}C Wiggles and Variations in Solar Irradiance', *Phil. Trans. Roy. Soc.* **A330**, 547–560.

Willson, R. C. and Hudson, H. S.: 1988, 'Solar Luminosity Variations in Solar Cycle 21', *Nature* **332**, 810–812.

Willson, R. C. and Hudson, H. S.: 1991, 'The Sun's Luminosity over a Complete Solar Cycle', *Nature* **351**, 42–44.

Zielinski, G. A.: 1995, 'Stratospheric Loading and Optical Depth Estimates of Explosive Volcanism over the Last 2100 Years Derived from the Greenland Ice Sheet Project 2 Ice Core', *J. Geophys. Res.* **100**, 20,937–20,955.

(Received 5 December 1997; in revised form 16 February 1999)